Acc. Chem. Res. **1998,** *31,* 18−25

Oxygen Production in Nature: A Light-Driven Metalloradical Enzyme Process

CECILIA TOMMOS†

Department of Biochemistry, Arrhenius Laboratories for Natural Sciences, Stockholm University, S-10691 Stockholm, Sweden

GERALD T. BABCOCK*

Department of Chemistry, Michigan State University, East Lansing, Michigan 48824

Received March 13, 1997

Introduction

Dioxygen is thermodynamically hot but kinetically cool, which makes it an ideal reagent for maximizing biological free energy production and for carrying out difficult chemical transformations in enzyme active sites.[1] The widespread use of dioxygen in biological catalysis has led to an enzyme classification scheme — monooxygenases, dioxygenases, oxidases — that is based on the specifics of the chemistry in which O_2 participates. Examples of the remarkable utility of dioxygen in biology abound and include its use in maximizing ATP production in aerobic respiration, in C−H bond activation in the P450 enzymes and methane monoxygenases, and in the degradation of important biomaterials such as lignin.

Although nature has devised a multitude of mechanisms by which to activate dioxygen for useful chemistry, only one system, Photosystem II (PSII) in plants and algae, has evolved that has the capacity to lift water out of its thermodynamic well to generate dioxygen. This singular development provided photosynthetic organisms with an abundant and ubiquitous substrate for growth and diversification. The molecular mechanism by which PSII is able to strip hydrogen atoms from water and release O_2 as waste is coming into view. In this article, we review the physical structure and energetics of PSII. We then discuss and analyze a metalloradical enzyme mechanism for the water-oxidation process it catalyzes.

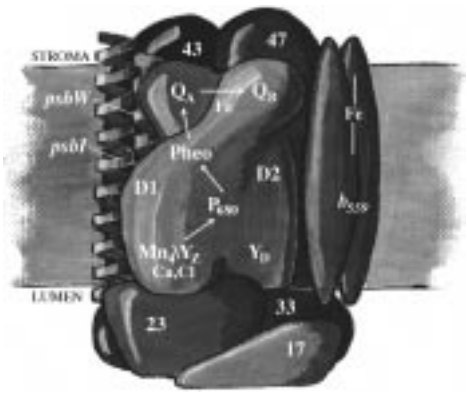

FIGURE 1. Major polypeptides and redox components in PSII.

Physical Structure of Photosystem II and an Overview of Water Oxidation

PSII occurs as a multi-subunit, membrane-spanning complex in the thylakoid membrane. Figure 1 shows a scheme of its reaction center that includes a number of the polypeptides and redox cofactors that are essential to the photochemistry and subsequent electron- and proton-transfer reactions that precede oxygen evolution.[2] Light absorption by the specialized chlorophyll complex, P680, generates a charge-separated state, $P680^+Q_A^-$, that is stable to recombination for ~200 μs. Reduction of $P680^+$ by a redox-active tyrosine Y_Z, Y161 of the D1 polypeptide, is fast and outcompetes the wasteful charge-recombination process. Electron transfer from Q_A to the secondary acceptor, Q_B, and concomitant protonation mobilize the hydroquinone for electron delivery to Photosystem I and, eventually, the CO_2-fixing reactions of the Calvin cycle.

Y_Z deprotonates as it reduces $P680^+$ to produce the neutral $Y_Z^\bullet$ radical.[2a,3] Reduction and reprotonation of $Y_Z^\bullet$ occur from water and the tetranuclear $(Mn)_4$ complex that provides the substrate-binding sites in the water-splitting complex. Recent work has shown that the tyrosine, the $(Mn)_4$ cluster, and the other two cofactors essential for water oxidation, Ca^{2+} and Cl^-, are likely to function as a single catalytic center in forming the oxygen-evolving complex (OEC) of PSII,[4,5] as discussed below.

Each photon-absorption and charge-separation event in PSII provides only a single oxidizing equivalent to the OEC. Since each PSII unit functions independently in catalyzing the four-electron water-splitting process,[2b] intermediate oxidation states of the OEC must exist and be stable over a reasonable time period. Kok summarized these mechanistic aspects of the water-oxidation process

Cecilia Tommos studied in the Department of Biochemistry and presented her Ph.D. thesis in 1997 at Stockholm University on the topic of photosynthetic water oxidation. Her research as a graduate student was performed with Stenbjörn Styring in Sweden and in collaboration with Gerald Babcock at Michigan State University. She recently joined Leslie Dutton at the Johnson Research Foundation, University of Pennsylvania, as a STINT postdoctoral fellow. Her current project is aimed at studying amino-acid-based redox chemistry by means of *de novo* protein synthesis.

Gerald T. Babcock was born and raised in Minnesota and did his undergraduate work at Creighton University in Omaha, Nebraska. He received his Ph.D. with Ken Sauer at the University of California at Berkeley and was an NIH postdoctoral Fellow with Graham Palmer at Rice University. Currently, he is Professor of Chemistry and Chairman at Michigan State University in East Lansing. He is an Associate Editor of *Annual Reviews of Physical Chemistry* and on the editorial boards of *Biochemistry* and the *Journal of Biological Chemistry*. Research in his laboratory focuses on using biochemical and spectroscopic techniques to understand the coupling between proton and electron motion in the bond-breaking and bond-forming reactions that accompany oxygen reduction to water in oxygen-metabolizing metalloproteins and oxygen production from water in the photosynthetic process.

† Present address: The Johnson Research Foundation, Department of Biochemistry and Biophysics, University of Pennsylvania, Philadelphia, PA 19104.

S0001-4842(96)00018-0 CCC: $15.00
Published on Web 01/20/1998

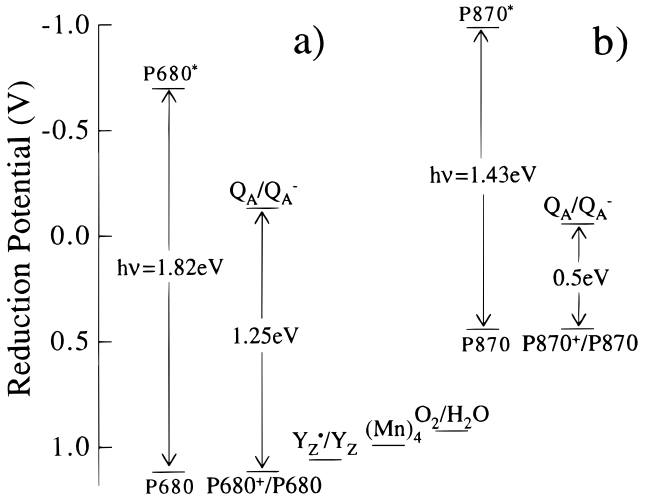

FIGURE 2. Photon absorption and charge separation energetics in (a) PSII and (b) photosynthetic bacterial reaction centers. For PSII, the O_2/H_2O couple at pH 5.0 and the cofactors involved in water splitting are shown.

by postulating the S-state notation in which the number of oxidizing equivalents stored in the OEC is denoted as S_n. The photochemistry/oxidizing equivalent accumulation process can thus be described as follows:

$$S_n\ P680\ Q_AQ_B \xrightarrow{h\nu} S_n\ P680^+\ Q_A^-Q_B \rightarrow S_{n+1}\ P680\ Q_AQ_B^-$$

Only when the S_4 state is reached does water oxidation occur.

Energetics in PSII Photochemistry and Water Oxidation

There are stringent energetic constraints on PSII that provide insight into viable mechanisms for water oxidation. Figure 2 compares the photochemical energetics of PSII with that of reaction centers from photosynthetic purple bacteria.[2a] The latter, for which detailed crystallographic information is available, has structural and functional analogies to PSII and is often used as a template in discussing PSII operation.[6] This approach has clear predictive power, as demonstrated by similarities in the quinone regions of the two photosystems and in the extension of C_2 symmetry themes to PSII.

Nonetheless, there are key differences. As Figure 2 shows, the efficiency of the conversion of photon energy into chemical potential is only 35% in the bacterial system, whereas it approaches 70% in PSII. This disparity arises from differences in the extent to which energy transfer and redox transitions are thermodynamically downhill in the two systems.[2a] The bacterial reactions are strongly driven, and the free energy changes enroute to a stable charge separation are large. An absorbed photon leads relentlessly to charge separation but with a considerable sacrifice in the chemical potential that is developed in the charge-separated state.

In PSII, weaker coupling occurs between chromophores and between redox cofactors, and the degree of irreversibility in each step lies less strongly in favor of product.

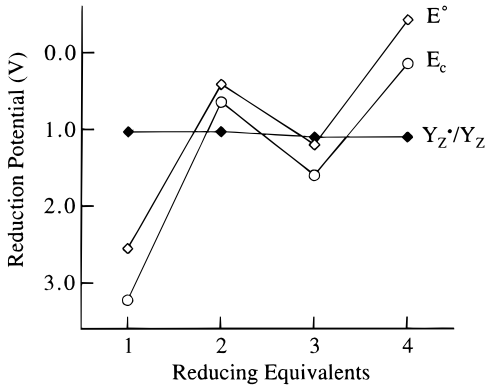

FIGURE 3. Reduction ($E°$; pH 5.0) and configurational potentials (E_c)[7] of the one-electron steps for $O_2 + 4H^+ + 4e^- \rightarrow 2H_2O$ relative to the reduction potential of $Y_Z^\bullet/Y_Z$.[2a]

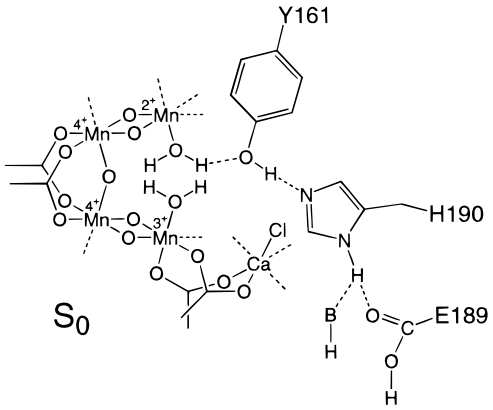

FIGURE 4. Proposed structure of the S_0 state in the OEC. The dotted lines to the metal centers indicate unspecified ligands or potentially unoccupied coordination sites.

Weak coupling carries through to the energetics of the water-splitting process itself. Although the quantum yield for O_2 production approaches unity, the overall free energy drop available to drive water oxidation in PSII is small, less than 200 mV per hydrogen atom stripped from water.[2a] Moreover, as Figure 3 shows, the individual steps in water oxidation vary significantly in their standard and configurational[7] reduction potentials. The first and third steps in the process are unfavorable, relative to the reduction potential available via $Y_Z^\bullet$, and a mechanism is necessary for leveling the free energy required, as has been discussed for O_2 reduction in cytochrome oxidase.[1]

Construction of the Catalytic Center for O_2 Evolution

Figure 4 provides a model for the oxygen-evolving complex that combines recent data in the literature with charge neutrality and proton current considerations.[5] Consensus that the manganese ions required for water splitting occur as a compact tetranuclear cluster is emerging.[2b,9] Yachandra *et al.* have interpreted their X-ray absorption data to indicate that the $(Mn)_4$ center has a C shape;[9a] in their structure, one can calculate that a distance of 5.5 Å separates the two manganese ions at the open end of the C. Although more controversial, the idea

that the Ca^{2+} and Cl^- cofactors are closely associated with the cluster has reasonable support.[2b,9a,10]

Site-directed mutagenesis has identified potential ligands to the $(Mn)_4/Ca^{2+}$ cluster, notably D170, H332, E333, H337, D342, and the carboxy terminus of A344, all in the D1 subunit of PSII.[3,11] Y_Z is close to the metal cluster,[4,12,13] and the proton-accepting base, which allows the functionally critical deprotonation of Y_Z during its oxidation by $P680^+$, is probably D1 H190.[3] To account for the appearance of protons in bulk phase on the time scale of Y_Z oxidation,[14] we suggested that H190 communicates with the inner thylakoid aqueous space by a hydrogen-bonded chain that may involve D1 E189,[3] either directly or by positioning water molecules in a hydrogen-bonded network analogous to those for the quinone sites in the bacterial reaction center[15] and for the binuclear center in cytochrome oxidase.[16]

In S_0, the valences of the four Mn ions sum to 13+.[2b,9a] We assign these to individual ions as 4+, 4+, 3+, and 2+; including the Ca^{2+}, the overall positive charge on the cluster in S_0 is 15+. This positive charge is exactly balanced by the five bridging oxos, the four carboxylates noted above, and the Cl^-. Moreover, these ligands are arranged in Figure 4 to provide local as well as overall charge neutrality in the cluster, i.e., so that each of the five metals has zero net charge. Electroneutrality in protein-bound metal centers is general[17] and follows from the energetic consequence of attempting to bury charge in regions of low dielectric.[18] The structures of many metalloprotein active sites, for example, that of the binuclear Mn cluster in arginase[19] and of the binuclear Fe centers in ribonucleotide reductase and methane monooxygenase,[20] demonstrate electroneutrality and its persistence during redox changes at the metal centers. Charge can apparently be tolerated on a metal/ligand cluster only when the site is sufficiently close to the surface of the protein to experience significant electrostatic screening from solvent water.[17] As the OEC is remote from bulk phase,[21] solvent screening will be muted, which reinforces the likelihood of the electroneutral structure shown in Figure 4. The operation of the metal-cluster/Y_Z site in oxygen evolution, described below, is driven to a large extent by the necessity of preserving overall electroneutrality in the complex during the S-state cycle.[5]

The Role of Y_Z in Water Oxidation and the S-State Cycle

Y_Z reduces $P680^+$ in nanoseconds to preserve the high quantum yield of charge separation in PSII and the highly oxidizing potential associated with $P680^+$. Recent work has extended the role of the tyrosine in PSII and implicated $Y_Z^\bullet$ intimately in the water-oxidizing chemistry itself.[4,5] By combining experimental data on $Y_Z^\bullet$ with emerging ideas on the function of the radical moiety in the general class of metalloradical enzymes, we suggested that Y_Z carries out hydrogen-atom abstraction from substrate water on each S-state transition.[5,22]

The rationale for this model is summarized in Figure 5. Figure 5A shows a mechanistic scheme for O_2-dependent metalloradical enzymes.[23] In this class of proteins, which includes galactose oxidase, ribonucleotide reductase, and prostaglandin synthase, the metal site activates dioxygen to produce a strong metal-bound oxidant. This activated oxygen species generates the amino acid radical by H-atom abstraction and the radical, in turn, abstracts a hydrogen atom from substrate to initiate catalysis. In casting PSII as a member of this class, we reverse the direction of the H-atom current (Figure 5B) and recognize that $P680^+$ is sufficiently oxidizing to serve as the thermodynamic sink in this process (Figure 5C). By postulating this mode of operation for PSII, clear analogies between it and other metalloradical enzymes emerge.[5,22]

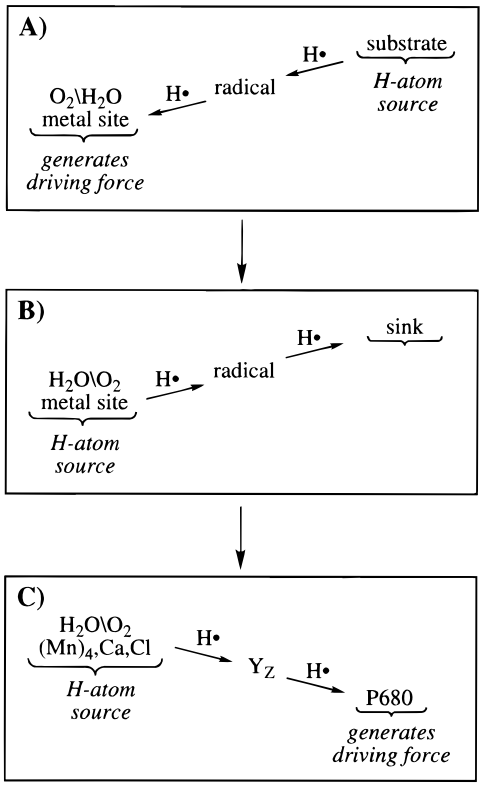

FIGURE 5. Schematic for casting PSII as a member of the metalloradical enzymes class.

The mechanistic view of PSII in Figure 5 meshes well with the structural model in Figure 4. The tyrosine is ideally positioned to promote forward electron transfer to $P680^+$, which is located 7−12 Å from it,[2a] while simultaneously undergoing deprotonation through the H190/E189/.../bulk phase pathway. This structure emphasizes the tight coupling in PSII between electron- and proton-transfer events that Krishtalik's work[8] virtually insists upon (see below). The proximity of Y_Z and the metal cluster is ideal for the H-abstraction function postulated for $Y_Z^\bullet$. We identify the two Mn ions at the open end of the C as the catalytic ions that bind substrate; H-atom abstraction by $Y_Z^\bullet$ from water bound terminally at these catalytic sites lies at the heart of each of the S-state transitions. Thus, the function of manganese in water oxidation becomes clear: it serves to bind substrate water, to delocalize oxidizing equivalents that are generated upon each H-atom abstraction, and to provide a template for

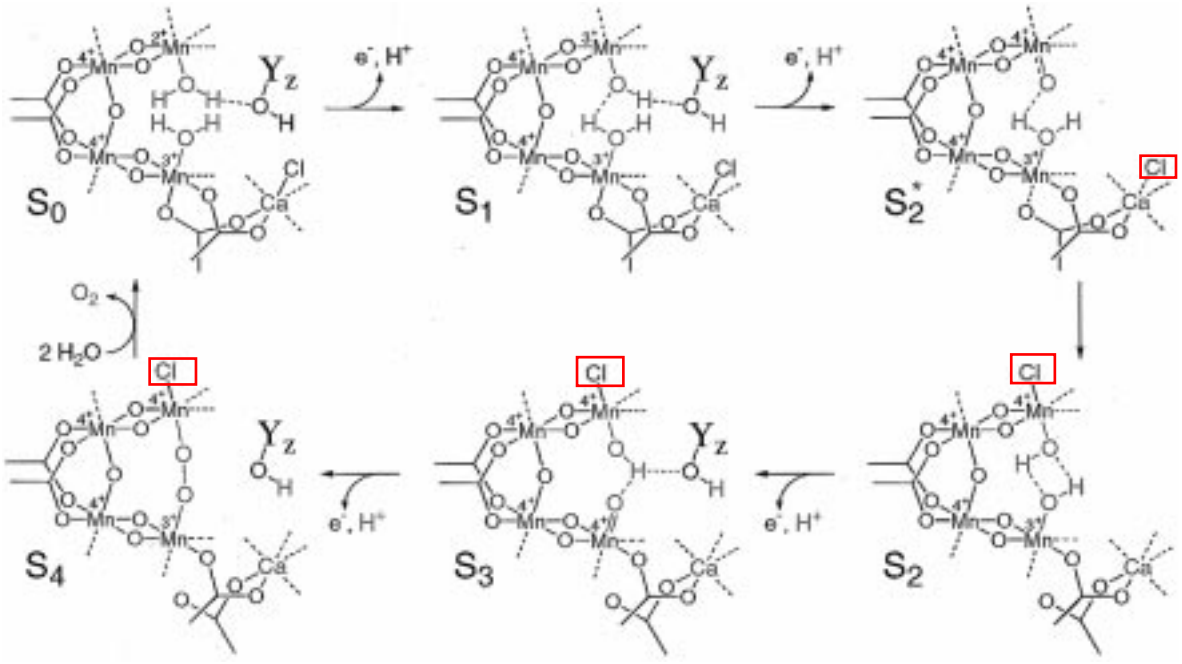

FIGURE 6. Model for the S-state cycle in PSII. The S_2* state occurs only transiently, and S_4 is unstable to O_2/S_0 production. In the three-dimensional structure, Cl^- may be closer to the upper catalytic site than is apparent in the scheme.

the critical O−O bond formation step. For the latter process, the 5.5 Å separation between the two catalytic ions is ideal.

Figure 6 presents a full S-state model based on the H-atom abstraction model. Although necessarily speculative in some aspects, it is consistent with a wide variety of observations on O_2 evolution. In S_0, the catalytic sites have 2+ or 3+ valences, and each is occupied by substrate water (see below). Photogeneration of $P680^+$ initiates the electron and proton motions that produce $Y_Z^{\bullet}$. The radical, in turn, abstracts an H atom from water bound to the upper catalytic ion to produce a ligated hydroxide; the oxidizing equivalent delocalizes to the Mn to oxidize it to 3+ in S_1. Upon a second photon absorption, $Y_Z^{\bullet}$ is formed and abstracts an H atom from the hydroxide to produce, transiently, an oxo species in the state labeled S_2*. For the d^4 Mn^{3+} ion in the S_1 state, Jahn−Teller (JT) distortions are in effect[24] and coordination to the axial position is expected to be weak or absent. Upon oxidation to the d^3 Mn^{4+} state in S_2*, the JT distortion is lifted. We postulate that relief of this distortion provides a driving force for Cl^- motion to the upper catalytic site. Ligation of the anion to the Mn^{4+} in S_2* increases the basicity of the oxo, relative to the water bound to the lower catalytic ion, which promotes a proton-transfer process to produce hydroxides at both catalytic centers. The coupled H^+/Cl^- motion is essential in positioning substrate in the higher S states[5c] and completes the $S_2^* \rightarrow S_2$ transition in Figure 6. Anion ligation may also prevent premature water oxidation.[25] Upon atom abstraction in $S_2 \rightarrow S_3$, the hydrogen-bonded oxo/hydroxyl species is formed. These ligands may equilibrate with a protonated peroxy species (Mn^{4+}═O···HO−Mn^{4+}),[26] although the equilibrium cannot lie too far right, as net manganese reduction does not take place on $S_2 \rightarrow S_3$.[9a,27] The final, O_2-producing transition proceeds according to the atom-abstraction/radical addition process discussed elsewhere.[22b] Upon completion of the cycle, Cl^- migrates back to the Ca site and two water molecules bind to reform the S_0 state.

The model in Figure 6 is structurally and mechanistically well founded. Moreover, it maintains overall cluster electroneutrality throughout the S-state cycle, which avoids the significant energetic penalties that would occur if charge were allowed to accumulate.[18] The model is conservative, as essentially the same chemistry occurs on each S-state transition, and minimal nuclear motion is required within the complex as it cycles through to produce O_2. The latter feature is of considerable importance, both in terms of the low driving force available to split water in PSII and of the high turnover number (up to 200 electrons s^{-1}) of the OEC.

Thermodynamics and Kinetics of the H-Atom Abstraction Process

The mechanism in Figure 6 must be shown to be thermodynamically feasible and kinetically competent. At first glance, the abstraction process presents a thermodynamic problem, as the bond dissociation energies (BDE's) for water (119 kcal/mol) and hydroxyl (102 kcal/mol) are significantly more exothermic than that for the tyrosyl O−H bond (87 kcal/mol).[28] Figure 7 summarizes the uncatalyzed situation. The formation of O_2 with a tyrosyl radical ($Y^{\bullet}(O)$) is exothermic as required, but only because of the strong exothermicity for forming the O═O bond in the final step; the individual H-abstraction steps are strongly endothermic.

$$^1/_2H_2O + Y^{\bullet}(O) \rightarrow {}^1/_4O_2 + Y(OH) \qquad (1)$$

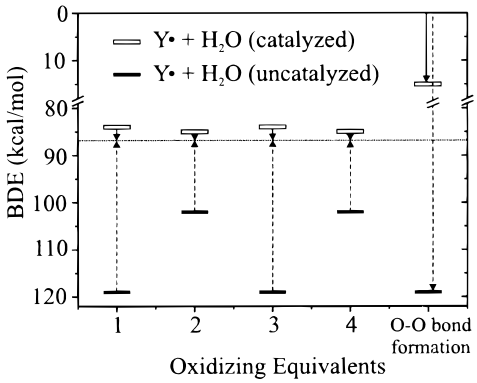

FIGURE 7. Comparison of the BDE's for water, free in solution[28b] [$Y^{\bullet} + H_2O$ (uncatalyzed)], and when complexed by a manganese ion[31] [$Y^{\bullet} + H_2O$ (catalyzed)]. The horizontal line represents the BDE for the tyrosine O−H bond.[28a] The vertical arrows show BDE differences between substrate water or hydroxyl O−H bonds and the tyrosyl O−H. The upward arrows, for the uncatalyzed case, indicate that atom abstraction by the tyrosyl radical is endothermic; the downward arrows, for the catalyzed case, indicate the exothermicity of abstraction by the tyrosyl radical. Two cycles, i.e., the process for two water molecules, are shown to demonstrate the energetics of O_2-bond formation as the right-most downward arrows.

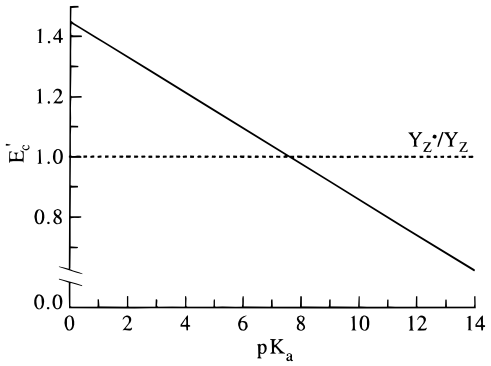

FIGURE 8. Configurational potential for the coupled proton/electron transfer in reaction 3 as a function of the pK_a of the base (solid line, see eq 4). The dashed line shows the configurational potential for the reduction of $Y_Z^{\bullet}$.

But, these energetics change radically when water is ligated to manganese.[29−31] The BDE's for H-atom abstraction drop for both water and hydroxide and occur in the 77−87 kcal/mol range (Figure 7), consistent with the essentially thermoneutral character of the $Y_Z^{\bullet}S_n$ transitions. The individual S-state transitions are now thermodynamically appropriate, and the O═O bond forming step is less strongly driven.

In radical-driven atom abstraction processes, entropic factors are close to zero,[32] which supports Mayer's emphasis on the predictive utility of BDE differences in radical reactions.[29] The importance of the energy release during the $Y_Z^{\bullet}$ O−H bond forming process and the nulling of entropic effects dovetail well with Krishtalik's analysis of O_2 evolution.[8] He noted that the configurational potential for the four-electron water-oxidation process

$$^1/_2H_2O = {}^1/_4O_2 + H^+ + e^- \qquad (2)$$

is 1.401 eV, which is significantly greater than the driving potential of 1.12 eV available from the reduction of $P680^+$. Accordingly, he concluded that water oxidation in PSII, in the absence of additional favorable processes, is not kinetically competent.

This realization led him to examine ways by which the OEC coupled further reactions to the fundamental redox chemistry in reaction 2. He quickly eliminated two such possibilities by showing that binding the oxidized oxygen-containing product species or beginning the reaction with hydroxide rather than water is ineffectual. However, protonation of a base (X^-) as the redox chemistry in (2) occurs, i.e.,

$$^1/_2H_2O + X^- = {}^1/_4O_2 + XH + e^- \qquad (3)$$

is more fruitful. His analysis showed that proton-binding affects the configurational potential as follows:

$$E_c' = E_c + {}^1/_2E_{H_2O} - [0.059(pK_a - \log \chi_{H^+})] \qquad (4)$$

where E_c is the configurational potential for (2) (1.401 V), E_{H_2O} is the binding energy of H_2O in the OEC, pK_a is that for the base in (3), and χ_{H^+} is the mole fraction of protons at pH 0 (1/55.5). With a reasonable binding energy for water (0.3 eV), a graphical analysis of eq 4 shows that E_c' drops to values below that of $Y_Z^{\bullet}/Y_Z$ for pK_a's for XH/X^- greater than 7.5 (Figure 8).

If the pK_a of XH/X^- in (3) approaches that of bulk solution, however, it is substantially protonated prior to the electron transfer and, thus, unavailable as a proton acceptor. If the pK_a is decreased to overcome this, the effect of the coupled protonation on the configurational potential is diminished and E_c' rises. To circumvent this difficulty, Krishtalik suggested redox-linked dissociation of a manganese ligand, possibly a semiquinone, to provide an acid/base function whose pK_a was coupled to the electron transfer in (2). This mechanism now appears unlikely, as quinones are not associated with the OEC, and there are no data to support the idea of redox-linked ligand dissociation on each S-state transition.

The tyrosyl radical in Figures 4 and 6, however, fulfills Krishtalik's criteria precisely. Upon oxidation by $P680^+$, the tyrosyl proton is sloughed from the site, owing to the low pK_a ($\lesssim -2$) of the cation radical, to generate $Y_Z^{\bullet}$. Its subsequent rereduction by H-atom transfer from substrate water/hydroxide regenerates the tyrosine form with pK_a $\sim$ 9. Within the context of (3), this pK_a is the operational value. We can represent the reaction sequence involved as

$$Y_Z^{\bullet} + e^- \leftrightarrow Y_Z^- \qquad (a)$$

$$^1/_2H_2O + Y_Z^- \leftrightarrow {}^1/_4O_2 + Y_Z + e^- \qquad (b)$$

$$^1/_2H_2O + Y_Z^{\bullet} \leftrightarrow {}^1/_4O_2 + Y_Z \qquad (\text{net}) \qquad (5)$$

where Y_Z represents the reduced, protonated tyrosine species. The high pK_a for Y_Z/Y_Z^- reduces the configurational potential for step b to ~0.9 V (Figure 8), and the

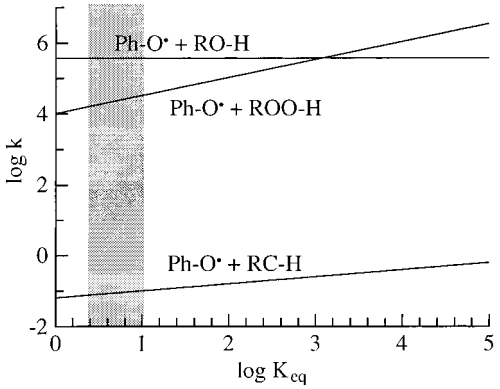

FIGURE 9. Linear free-energy relationships for H-atom abstraction processes according to eqs 6−8. The shaded area represents the range of the equilibrium constants for the $S_nY_Z^{\bullet} \leftrightarrow S_{n+1}Y_Z$ reactions of the S-state cycle.[2]

configurational potential available in the reduction of $Y_Z^{\bullet}$ (∼1.0 V) becomes sufficient to drive the net process in (5). Thus, the Krishtalik analysis within the context of the metalloradical mechanism for water oxidation (5) converges with the BDE data for reaction 1.

The S-state transitions have rates of 10^3-10^4 s^{-1}, despite the weak driving forces available.[2] Can the metalloradical−enzyme mechanism account for these kinetics? For atom-abstraction processes, linear free energy relationships (LFE's) that relate the difference in BDE's for the reactant and product bonds (ΔBDE) to the rate of the abstraction process are available. Mahoney and DaRooge,[32] for example, have studied the relationship between rate and equilibrium for H-atom abstraction from both O−H and C−H bonds by phenoxyl radicals (PhO•). For phenoxyls reacting with organic hydroperoxides (ROO−H), they developed the LFE

$$\log k = 4.0 + 0.51 \log K_{eq} \qquad (6)$$

where k is the second-order rate constant for abstraction and K_{eq} is the equilibrium constant for the abstraction process. For the analogous reactions of phenoxyl radicals with substituted phenols (RO−H), the abstraction rate was independent of K_{eq}

$$\log k = 5.65 \pm 0.15 \qquad (7)$$

where k is defined as in (6). Finally, for phenoxyl radicals abstracting H atoms from hydrocarbon C−H bonds, the relationship

$$\log k = -1.2 + 0.2 \log K_{eq} \qquad (8)$$

was observed, where k and K_{eq} are defined as for (6). Figure 9 summarizes these LFE's graphically. Ingold and co-workers recently presented a study of phenoxyl radical reactivity consistent with the above.[33]

These LFE's led to two important conclusions. First, phenoxyl radicals are significantly, by 4−5 orders of magnitude, more reactive in abstracting H atoms from O−H bonds than from C−H bonds. Thus, assessment of the kinetic competence of the mechanism in Figure 6 on the basis of LFE's derived from C−H bond hydrogen-atom abstraction rates is not well founded. Second, if we take the effective concentration of the reacting partners in the OEC, Y_Z and Mn^{n+} $H_2O(OH)$, as 10 M[25b] and equilibrium constants in the range 2−10 for the individual S-state transitions,[2] rate constants for these transitions of $\geq 10^5$ s^{-1} are predicted (Figure 9). The lower rates, 10^3-10^4 s^{-1}, observed for $S_nY_Z^{\bullet} \rightarrow S_{n+1}Y_Z$ may reflect metal ligation or protein constraints. Overall, the organic radical reactivity data show that Y_Z is kinetically competent to carry out the H-atom abstraction processes we postulate.

The $Y_Z^{\bullet}$ species could provide a hazard in PSII, as the BDE's of various protein C−H bonds are close to the tyrosyl O−H bond.[28,34] Thus, destructive side reactions become possible. The number of nonexchangeable protons in the vicinity of the radical, however, is low in Mn-containing PSII preparations, which suggests that the catalytic site is protected from spurious reactions by isolating $Y_Z^{\bullet}$ from C−H bonds with which it could react.[35]

Electroneutrality and Substrate Binding

Britt reviewed work aimed at understanding the steps in the S-state cycle at which substrate water/hydroxide binds,[2b] and concluded that water or hydroxide is already ligated in the lower S states. This conclusion is consistent with recent ENDOR measurements[36] and suggests that two substrate molecules reload directly following O_2 formation and are bound at the catalytic Mn sites in S_0 (Figure 6).

Pecoraro and co-workers studied the acid/base properties of Mn model compounds.[30,37] This work, in combination with the likelihood of electroneutrality in the OEC, provides insight as to the protonation state of the bound waters, i.e., whether substrate ligates as water or hydroxide. Table 1 summarizes pK_a data for a variety of binuclear and mononuclear Mn complexes. From this compilation, several trends emerge. First, overall cluster charge is critical in determining acid/base properties. Introducing a charge as the result of deprotonation, whether at bridging (compounds **1** and **5**) or terminal (**9**) positions, requires extremely basic conditions (pK_a's 19−25), and the oxos become progressively more acidic as the total charge in the cluster increases. Second, the manganese valence, within the III and IV valence set that is most relevant to the OEC, has little effect on pK_a, provided the charge change upon deprotonation is the same (**2** and **3**). Third, solvent dielectric effects are substantial and, as noted in the discussion above on electroneutrality, the effects of charge are muted in more polar environments (**2**−**4** and **6** in CH_3CN versus **7** and **8** in H_2O). Fourth, although bridging oxos appear to be more basic than terminal oxygens under the same Δq conditions (e.g., **1** and **5** versus **9**), this apparent trend is complicated by dissimilar dielectric conditions.

From Table 1, we conclude that, if the overall complex is charge neutral in S_0, then the ligated form of the substrate is undoubtedly H_2O. Even if the OEC carried a charge of 1+ in S_0, water would still be the preferred ligand, as the pK_a's for **2**, **6**, and **10** are all greater than 10. Only with an overall cluster charge greater than 2+

Table 1. pK_a's of Selected Dimanganese Compounds

no.	compd	Δq[a]	pK_a	ref
	A. Bridging Oxos			
1	$[Mn^{IV}Mn^{III}(salpn)_2]$[b] ($\mu$-O, μ-OH)	0 → 1−	24.5 ± 0.7[c]	30a
2	$[Mn^{IV}Mn^{IV}(salpn)_2]$ (μ-O, μ-OH)	1+ → 0	13.4 ± 0.2[c]	30a
3	$[Mn^{IV}Mn^{III}(salpn)_2]$ (μ-OH, μ-OH)	1+ → 0	13.0[c]	30a
4	$[Mn^{IV}Mn^{IV}(salpn)_2]$ (μ-OH, μ-OH)	2+ → 1+	6.5[c]	30a
5	$[Mn^{IV}Mn^{III}$(3,5-diCl(salpn)$_2$] (μ-O, μ-OH)	0 → 1−	20.5 ± 1.0[c]	30a
6	$[Mn^{IV}Mn^{IV}$(3,5-diCl(salpn)$_2$] (μ-O, μ-OH)	1+ → 0	10.8 ± 0.3[c]	30a
7	$[Mn^{III}Mn^{III}bpy_2]$[d] (μ-O, μ-OH)	3+ → 2+	11.0[e]	37
8	$[Mn^{IV}Mn^{III}bpy_2]$[d] (μ-O, μ-OH)	4+ → 3+	2.3[e]	37
	B. Terminal Oxos			
9	$[Mn^{III}Mn^{III}L_2]$[f] (H_2O)	0 → 1−	19[g]	30b
10	$[Mn^{IV}Mn^{III}L_2]$ (H_2O)	1+ → 0	11	30b
11	$[Mn^{IV}Mn^{IV}L_2]$ (H_2O)	2+ → 1+	<0	30b
	C. Mononuclear Complexes			
12	$Mn^{II}(H_2O)_6$	2+ → 1+	10.6	42
13	$Mn^{III}(H_2O)_6$	3+ → 2+	−0.6	42
14	$HMnO_4^-$	1− → 2−	10.5	29

[a] The Δq is the net change in charge on the complex as it undergoes deprotonation. [b] salpn = *N*,*N*′-bis(saliclidene)-1,3-propanediamine. [c] Measured in CH_3CN or corrected to reflect pK_a's in CH_3CN. [d] bpy = 2,2′-bipyridine. [e] Measured in H_2O. [f] L = 2-hydroxy-1,3-bis(salicylamino)propane. [g] Measured in 16 M water/CH_3CN.

in the S_0 state, which is unusual in protein-bound clusters,[17] would we expect to ligate hydroxide in effective competition with water. Thus, the model compound work provides a strong basis for H_2O as the ligated substrate form.

Calcium, Chloride, and Proton Currents

The H-atom abstraction model predicts proton release upon each S-state transition with release kinetics on the time scale of Y_Z oxidation. This behavior is observed in a variety of thylakoid, PSII-membrane, and PSII-core preparations.[14] Moreover, in PSII-core particles, which are devoid of a number of ancillary PSII polypeptides, Junge and co-workers have found a pH-independent 1:1:1:1 H^+ release pattern.[14b] In less resolved preparations, the proton-release pattern is more intricate, which is usually taken to reflect a combination of substrate proton release and pH- and S-state-dependent redox Bohr effects.[14] In addition, a persistent electrochromism accompanies the $S_1 \rightarrow S_2$ transition, which is reversed on the $S_3 \rightarrow S_4 \rightarrow S_0$ transition.[2c] These band shifts are not coupled to the proton-release pattern.[14b] Consistent with the arguments above on electroneutrality, we attribute both the persistent electrochromic effects and the Bohr effects on H^+ release to internal charge rearrangement within the OEC, rather than to the creation of a naked charge.

The S-state cycle in Figure 6 accounts for this internal charge rearrangement. In S_0 and S_1, local electroneutrality is maintained about each of the metal centers in the OEC. However, with the generation of the transient oxo species in S_2*, we postulate coupled H^+ and Cl^- motion to form an S_2 state competent to complete the S cycle. In S_2, local neutrality is maintained about the upper catalytic Mn ion (two bridging oxos, the Cl^- and the OH^-), but a $-^1/_2/+^1/_2$ dipole is introduced between the lower catalytic Mn and the Ca. We attribute the local electrochromism and the Bohr effects to this internal charge rearrangement. Cl^- motion is clearly implicated in these phenomena, as neither is observed on the $S_1' \rightarrow S_2'$ transition in Cl^--depleted material,[38] even though Mn oxidation occurs.[39] Moreover, the charge rearrangement upon S_2 formation may rationalize the decrease in the rate of Y_Z oxidation by $P680^+$ in the higher S states.[2c]

By postulating an essential function for Cl^- in positioning substrate for H-atom abstraction on $S_2 \rightarrow S_3$ and $S_3 \rightarrow S_4 \rightarrow S_0$, Figure 6 accounts for a variety of observations on the roles of Cl^- and Ca^{2+}. Thus, Ca^{2+} serves as an anchor for Cl^- within the catalytic site, consistent with the ordered binding of these two cofactors[40] and the slow Cl^- release kinetics.[41] The 17 and 24 kDa polypeptides play a role in the latter phenomenon[2] and, together, are likely to prevent Cl^- association/dissociation from rate-limiting water oxidation. Under conditions of Cl^- or Ca^{2+} depletion, the S-state cycle can advance one step beyond the S_1 state; subsequent illumination generates the modified $S_2Y_Z^\bullet$ EPR signal.[4,12] The linked action of Ca^{2+} and Cl^- in controlling proton motion for the formation of the functional S_2 state provides a rationale for the susceptibility of the oxygen-evolving complex to produce this modified S_2 state, which cannot advance further in the S-state cycle,[43] under a variety of inhibitory conditions.

Conclusions

The oxygen-evolution chemistry in PSII arises from a remarkable enzymatic structure that operates under stringent energetic and kinetic constraints. We have set out many of these and have described a mechanism that operates within the confines they impose. The mechanism survives thermodynamic and kinetic tests, as described above, and provides a chemical basis for the formation of the O═O bond.[22b] A specific structure for the $(Mn)_4$ cluster has been adopted in developing this mechanism, and we have proposed roles for Ca^{2+} and Cl^- within the context of hydrogen-atom abstraction chemistry. These aspects of the model are based on solid data from a variety of labs, but they continue to attract intense experimental scrutiny; the details of these facets of Figure 6 may evolve. Nonetheless, the concepts that underlie the mechanism — H-atom abstraction on each S-state transition, the importance of overall charge neutrality, and the functional association of Y_Z, $(Mn)_4$, Ca^{2+}, and Cl^- in forming a structurally compact water-splitting complex — are likely to persist and provide a solid basis for further effort to understand the chemistry that pumps O_2 into our atmosphere.

We thank Drs. Vince Pecoraro, Charlie Yocum, Jim Mayer, Curt Hoganson, Per Siegbahn, and Margareta Blomberg for insightful discussion and Hasse Bergman for his artistic skills in drawing Figure 1.

References

(1) Babcock, G. T.; Wikström, M. *Nature* **1992**, *356*, 301−309 and references therein.

(2) (a) Diner, B. A.; Babcock, G. T. In *Oxygenic Photosynthesis: The Light Reactions*; Ort, D. R., Yocum, C. F., Eds.; Kluwer: Dordrecht, The Netherlands, 1996; pp 213−247. (b) Britt, R. D. *Ibid*. pp 137−164. (c) Witt, H. T. *Ber. Bunsen-Ges. Phys. Chem*. **1996**, *100*, 1923−1942.

(3) Chu, H.-A.; Nguyen, A. P.; Debus, R. J. *Biochemistry* **1995**, *34*, 5839−5858 and references therein.

(4) (a) Gilchrist, M. L., Jr.; Ball, J. A.; Randall, D. W.; Britt, R. D. *Proc. Natl. Acad. Sci. U.S.A.* **1995**, *92*, 9545−9549. (b) Tang, X.-S.; Randall, D. W.; Force, D. A.; Diner, B. A.; Britt, R. D. *J. Am. Chem. Soc.* **1996**, *118*, 7638−7639.

(5) (a) Tommos, C.; Tang, X.-S.; Warncke, K.; Hoganson, C. W.; Styring, S.; McCracken, J.; Diner, B. A.; Babcock, G. T. *J. Am. Chem. Soc.* **1995**, *117*, 10325−10335. (b) Hoganson, C. W.; Lydakis-Simantiris, N.; Tang, X.-S.; Tommos, C.; Warncke, K.; Babcock, G. T.; Diner, B. A.; McCracken, J.; Styring, S. *Photosynth. Res.* **1995**, *46*, 177−184. (c) Tommos, C. Ph.D. Thesis, Stockholm University, Stockholm, Sweden, 1997.

(6) Michel, H.; Deisenhofer, J. *Biochemistry* **1988**, *27*, 1−7.

(7) Krishtalik[8] defined the configurational component of the free energy (reduction potential) for water oxidation as the driving force required independent of proton dilution (entropic) effects in bulk solution. His analysis provides insight into driving forces within the active site and gives access to the kinetic competence of proposed reaction steps.

(8) Krishtalik, L. I. *Biochim. Biophys. Acta* **1986**, *849*, 162−171. (b) Krishtalik, L. I. *Bioelectrochem. Bioenerg.* **1990**, *23*, 249−263.

(9) (a) Yachandra, V. K.; Sauer, K.; Klein, M. P. *Chem. Rev.* **1996**, *96*, 2927−2950. (b) Riggs-Gelasco, P. J.; Mei, R.; Yocum, C. F.; Penner-Hahn, J. E. *J. Am. Chem. Soc.* **1996**, *118*, 2387−2399. (c) But, see: Åhrling, K. A.; Pace, R. J. *Biophys. J.* **1995**, *68*, 2081−2090.

(10) (a) Riggs-Gelasco, P. J.; Mei, R.; Ghanotakis, D. F.; Yocum, C. F.; Penner-Hahn, J. E. *J. Am. Chem. Soc.* **1996**, *118*, 2400−2410. (b) But, see: Booth, P. J.; Rutherford, A. W.; Boussac, A. *Biochim. Biophys. Acta* **1996**, *1277*, 127−134.

(11) (a) Nixon, P. J.; Chisholm, D. A.; Diner, B. A. In *Plant Protein Engineering*; Shewry, P. R., Gutteridge, S., Eds.; Cambridge University Press: U.K., 1992; pp 93−141. (b) Vermaas, W. *Annu. Rev. Plant Physiol. Plant Mol. Biol.* **1993**, *44*, 457−481. (c) Chu, H.-A.; Nguyen, A. P.; Debus, R. J. *Biochemistry* **1995**, *34*, 5859−5882.

(12) Boussac, A.; Zimmerman, J.-L.; Rutherford, A. W.; Lavergne, J. *Nature* **1990**, *347*, 303−306.

(13) (a) Force, D. A.; Randall, D. W.; Britt, R. D. *Biochemistry* **1997**, *36*, 12062−12070. (b) Lydakis-Simantiris, N.; Dorlet, P.; Ghanotakis, D.; Babcock, G. T. *Biochemistry*, submitted.

(14) (a) Lavergne, J.; Junge, W. *Photosynth. Res.* **1993**, *38*, 279−296. (b) Haumann, M.; Junge, W. In ref 2a, pp 165−192.

(15) Lancaster, C. R. D.; Michel, H.; Honig, B.; Gunner, M. R. *Biophys. J.* **1996**, *70*, 2469−2492.

(16) Iwata, S.; Ostermeier, C.; Ludwig, B.; Michel, H. *Nature* **1995**, *376*, 660−669.

(17) Lippard, S. J.; Berg, J. M. *Principles of Bioinorganic Chemistry*; University Science Books: U.S., 1994.

(18) Rich, P. R. In *Protein Electron Transfer*; Bendall, D. S., Ed.; BIOS Scientific Publishers Ltd.: Oxford, U.K., 1996; pp 217−248.

(19) Kanyo, Z. F.; Scolnick, L. R.; Ash, D. E.; Christianson, D. W. *Nature* **1996**, *383*, 554−557.

(20) Wallar, B. J.; Lipscomb, J. D. *Chem. Rev.* **1996**, *96*, 2625−2657 and references therein.

(21) (a) Koulougliotis, D.; Tang, X.-S.; Diner, B. A.; Brudvig, G. W. *Biochemistry* **1995**, *34*, 2850−2856. (b) Tommos, C.; McCracken, J.; Styring, S.; Babcock, G. T. *J. Am. Chem. Soc.*, submitted.

(22) (a) Babcock, G. T.; Espe, M.; Hoganson, C. W.; Lydakis-Simantiris, N.; McCracken, J.; Shi, W.; Styring, S.; Tommos, C.; Warncke, K. *Acta Chem. Scand.* **1997**, *51*, 533−540. (b) Hoganson, C. W.; Babcock, G. T.; *Science* **1997**, *277*, 1953−1956.

(23) (a) Frey, P. A. *Chem. Rev.* **1990**, *90*, 1343−1357. (b) Sigel, H.; Sigel, A. *Metal Ions in Biological Systems*; Marcel Dekker Inc.: New York, 1994.

(24) Manchandra, R.; Brudvig, G. W.; Crabtree, R. H. *Coord. Chem. Rev.* **1995**, *144*, 1−38.

(25) (a) Rutherford, A. W. *Trends Biochem. Sci.* **1989**, *14*, 227−232. (b) Rüttinger, W.; Dismukes, G. C. *Chem. Rev.* **1997**, *97*, 1−24.

(26) Renger, G. *Photosynth. Res.* **1993**, *38*, 229−247.

(27) (a) Ono, T.; Noguchi, T.; Inoue, Y.; Kusunoki, M.; Matsushita, T.; Oyanagi, H. *Science* **1992**, *258*, 1335−1337. (b) Dekker: J. P. In *Manganese Redox Enzymes*; Pecoraro, V. L., Ed.; VCH Publishers Inc.: New York, 1992; pp 85−103.

(28) (a) Lind, J.; Shen, X.; Eriksen, T. E.; Merényi, G. *J. Am. Chem. Soc.* **1990**, *112*, 479−482. (b) Lide, D. R. *CRC Handbook*; CRC Press: Boca Raton, FL, 1996.

(29) Gardner, K. A.; Mayer, J. M. *Science* **1995**, *269*, 1849−1851.

(30) (a) Baldwin, M. J.; Pecoraro, V. L. *J. Am. Chem. Soc.* **1996**, *118*, 11325−11326. (b) Caudle, M. T.; Pecoraro, V. L. *J. Am. Chem. Soc.* **1997**, *119*, 3415−3416.

(31) Blomberg, M. R. A.; Siegbahn, P. E. M.; Styring, S.; Babcock, G. T.; Åkermark, B.; Korall, P. *J. Am. Chem. Soc.* **1997**, *119*, 8285−8292.

(32) Mahoney, L. R.; DaRooge, M. A. *J. Am. Chem. Soc.* **1975**, *97*, 4722−4731.

(33) Foti, M.; Ingold, K. U.; Lusztyk, J. *J. Am. Chem. Soc.* **1994**, *116*, 9440−9447.

(34) Rauk, A.; Yu, D.; Armstrong, D. A. *J. Am. Chem. Soc.* **1997**, *119*, 208−217.

(35) Tommos, C.; McCracken, J. In preparation.

(36) (a) Fiege, R.; Zweygart, W.; Bittl, R.; Adir, N.; Renger, G.; Lubitz, W. *Photosynth. Res.* **1996**, *48*, 227−237. (b) But, see: Turconi, S.; MacLachlan, D. J.; Bratt, P. J.; Nugent, J. H. A.; Evans, M. C. W. *Biochemistry* **1997**, *36*, 879−885.

(37) Baldwin, M. J.; Gelasco, A.; Pecoraro, V. L. *Photosynth. Res.* **1993**, *38*, 303−308.

(38) Haumann, M.; Drevenstedt, W.; Hundelt, M.; Junge, W. *Biochim. Biophys. Acta* **1996**, *1273*, 237−250.

(39) Ono, T.; Nuguchi, T.; Inoue, Y.; Kusunoki, M.; Yamaguchi, H.; Oyanagi, H. *J. Am. Chem. Soc.* **1995**, *117*, 6386-6387.

(40) Yocum, C. F. In ref 27b, pp 71−83.

(41) Lindberg, K.; Andréasson, L.-E. *Biochemistry* **1996**, *35*, 14259−14267.

(42) Hawkes, S. J. *J. Chem. Educ.* **1996**, *73*, 516−517.

(43) Wincencjusz, H.; van Gorkom, H. J.; Yocum, C. F. *Biochemistry* **1997**, *36*, 3663−3670.

AR9600188